

pubs.acs.org/JPCC Article

Selective Hydrogenation of Acrolein on a Pd/Ag(111) Single-Atom Alloy Surface

Mark Muir, David L. Molina, Arephin Islam, Mohammed K. Abdel-Rahman, and Michael Trenary*



Cite This: J. Phys. Chem. C 2020, 124, 24271-24278



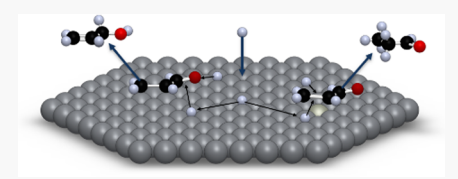
ACCESS

Metrics & More



3 Supporting Information

ABSTRACT: The hydrogenation of acrolein on the Ag(111) and Pd/Ag(111) single-atom alloy (SAA) surfaces was studied using temperature-programmed reaction spectroscopy. On Ag(111), the percent conversion of acrolein increased with increasing atomic hydrogen coverage. At an acrolein coverage of 0.17 ML followed by a low exposure to atomic hydrogen, the highest selectivity to 2-propenol was reached at 19%. However, increasing the acrolein coverage caused the selectivity to 2-propenol to decrease and the selectivity to propanal to increase to a maximum of 92%. In all cases,



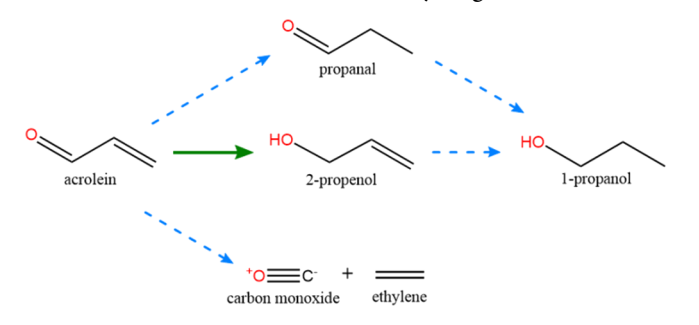
increasing atomic hydrogen exposure decreased the selectivity to 2-propenol. The selectivity to 1-propanol was constant at only 1%. Activity and conversion on the Ag(111) and Pd/Ag(111) SAA surfaces were compared for Pd coverages of 0.2, 0.5, and 0.9%. With increasing Pd coverage, the percent conversion increased while the selectivity to 2-propenol decreased. The selectivity toward 1-propanol only increased from 1 to 3% for the 0.9% Pd/Ag(111) SAA surface.

■ INTRODUCTION

Chemoselective hydrogenation of α , β -unsaturated aldehydes to the corresponding unsaturated alcohol is desirable in fine chemical production, pharmaceutical precursors, and the fragrance industry. However, hydrogenation at the C=C bond is thermodynamically favored and produces the undesired saturated aldehyde. To counter this reaction pathway, a suitable catalyst must be employed to promote hydrogenation at the C=O bond. The simplest α , β -unsaturated aldehyde, acrolein, has a low selectivity toward the desired product, 2-propenol, because the C=C group bonds to the catalyst surface and is readily hydrogenated. In addition, acrolein can undergo decarbonylation to ethylene and CO or decomposition to surface carbon and hydrogen over more reactive catalysts. Scheme 1 depicts the various reaction pathways of acrolein.

More active metals, such as Pt, Pd, Ni, and Ru, show higher conversions as these metals can readily dissociate H_2 , but at the

Scheme 1. Reaction Pathways for Acrolein, Where the Green Arrow Indicates the Desired Hydrogenation Reaction



cost of lower selectivity toward unsaturated alcohols.^{7–9} Using DFT calculations, Tuokko et al. found that the selective hydrogenation of acrolein on Pd(111) and Pt(111) is governed by steric effects of the adsorbate.¹⁰ They show that with increasing acrolein coverage, the selectivity decreases.

In contrast, less reactive metals such as Ag, Au, and Cu, should exhibit weaker binding to α,β -unsaturated aldehydes, resulting in a higher selectivity to the unsaturated alcohol. Although they show high selectivity, they also exhibit weak activity due to poor hydrogen activation. Furthermore, atomic hydrogen is generally weakly bound on these metals and may desorb as H2 at temperatures below that required for hydrogenation. Bron et al. studied the pressure effects of acrolein hydrogenation on silica-supported Ag nanoparticles at total pressures of 2 mbar to 20 bar at a constant H₂/acrolein ratio of 20:1 and found that 2-propenol was favored (up to 42%) at higher pressures. 11 Claus et al. used Ag/SiO₂ and Ag/ TiO2 nanoparticles to observe the hydrogenation of crotonaldehyde as a function of particle size to the desired product, crotyl alcohol.¹² They observed a selectivity of 59% for the silica-supported Ag independent of the size range from 3.7 to 6.3 nm and less selectivity below that range.

In surface science experiments on Ag(111), Brandt et al. observed selectivity toward crotyl alcohol as high as 95% for 0.3 monolayer (ML) of crotonaldehyde and 0.66 ML of $\rm H_a$. ¹³

Received: September 4, 2020 Revised: September 23, 2020 Published: October 23, 2020





In an earlier near-edge X-ray absorption fine structure (NEXAFS) and temperature-programmed reaction spectroscopy (TPRS) study of acrolein hydrogenation on Ag(111), Brandt et al. concluded that molecular orientation on the surface dictates selectivity. 14 With increasing acrolein coverage from 0.45 to 0.85 ML, they showed that the C=C bond tilts from 6 to 12° while the C=O bond remains unchanged at a 2° tilt from the surface. They concluded that the increased tilt of the C=C bond makes it less vulnerable to reaction with atomic hydrogen, thus favoring the desired product, 2propenol, at higher acrolein coverages. Similar considerations apply to the subsequent hydrogenation of 2-propenol. They found that at low H-atom coverages, the C=C bond of 2propenol was tilted away from the surface, inhibiting further hydrogenation to propanol. At higher H-atom coverages, 2propenol was oriented with the C=C bond nearly parallel to the surface, which favored hydrogenation. They observed a 27% selectivity toward 2-propenol at 30% conversion at the highest H atom coverage and an acrolein coverage of 0.6 ML.¹⁴

The structure of acrolein adsorbed on Ag surfaces has also been studied with reflection absorption infrared spectroscopy (RAIRS). ^{15,16} Fujii et al. observed that at low acrolein coverages on Ag films, the peaks for the out-of-plane modes were the most intense, implying that the molecule adsorbed parallel to the surface, in which case the C=C bond would presumably be involved in bonding to the Ag atoms. ¹⁵ Similar RAIRS results were obtained for acrolein on the Ag(111) surface. ¹⁶

Recently, novel bimetallic catalysts known as single-atom alloys (SAAs) have shown promise for selective hydrogenations. In an SAA, a catalytically active transition metal is doped at low concentrations into an inert coinage metal host such that the dopant is dispersed in the form of individual, isolated atoms in the surface layer. SAA catalysts combine the high reactivity of the dopant while maintaining the selectivity of the host metal. For example, dosing molecular hydrogen onto the Pd/Cu(111) surface has shown to dissociate H_2 at the palladium sites and cause spillover of H_2 atoms onto the Cu(111) surface. These weakly adsorbed H_2 atoms have been shown to participate in selective hydrogenation of unsaturated hydrocarbons on the Pd/Cu(111) SAA surface. H_2 18,19

In previous work, we characterized the Pd/Ag(111) SAA surface using RAIRS and TPD of adsorbed CO.²⁰ Although we assumed that H₂ dissociated at the Pd sites, we did not observe any H atom spillover to the Ag(111) sites.²⁰ Recent work on higher coverages of Pd on Ag(111) shows that H-atom spillover from Pd islands to the Ag(111) surface can occur under special circumstances.²¹ The dynamics of Pd- and Agatom exchange between Pd islands and the Ag(111) substrate has recently been studied with machine learning molecular dynamics.²² Aich et al. studied the hydrogenation of acrolein over a PdAg SAA nanoparticle catalyst supported on SiO2 in a fixed-bed continuous flow reactor. 23 They observed a 37% selectivity to 2-propenol with an 8% Ag/SiO2 catalyst and a 31% selectivity with 0.01% Pd + 8% Ag/SiO₂; however, the alloy shows a doubling in reaction rate. They concluded that the presence of Pd facilitates hydrogen dissociation and selectivity at very dilute concentrations, although the Pd will ultimately dominate the observed reactivity at higher concentrations. Their work suggests that PdAg SAAs may offer significant advantages as selective hydrogenation catalysts.²³ It is therefore important to establish if a higher selectivity and activity for acrolein hydrogenation can be achieved over the Pd/Ag(111) SAA compared to what Brandt et al. achieved over Ag(111).¹⁴ Here, we use TPRS to study the selectivity of acrolein hydrogenation to 2-propenol on well-defined surfaces of Ag(111) and a Pd/Ag(111) SAA.

■ EXPERIMENTAL METHODS

The experiments were performed in an ultrahigh vacuum (UHV) chamber with a base pressure of 1×10^{-10} Torr. The chamber is equipped with a PHI 10–155 cylindrical mirror analyzer for Auger electron spectroscopy (AES), PHI 15–120 optics for low-energy electron diffraction (LEED), and a Hiden HAL201/3F quadrupole mass spectrometer for temperature-programmed reaction spectroscopy (TPRS) or temperature-programmed desorption (TPD). We designate the technique as TPD for experiments where molecules desorb without undergoing any surface chemical reactions and as TPRS where reactions do occur. The UHV chamber is coupled to a Bruker IFS-66v/s Fourier-transform infrared (FTIR) spectrometer. The incident and reflected IR beams enter and exit the UHV chamber through differentially pumped, O-ring-sealed KBr windows.

The mounting of the Ag(111) crystal has been described elsewhere. The crystal was cleaned with Ar sputtering (1 keV, 8 μ A) and annealing to 800 K. The cleanliness of the surface was determined using LEED and AES. The lack of a RAIRS peak at 85 K for CO on Pd sites confirmed the absence of Pd below the AES detection limit of approximately 1.5%. A homemade evaporator was used to deposit Pd onto the Ag(111) surface with the crystal held at 380 K. CO (99.99%), and hydrogen (99.999%) gases were obtained from Matheson Trigas and Praxair, respectively. Acrolein (96%, stabilized with hydroquinone, Alfa Aesar), 2-propenol (\geq 99%, Sigma Aldrich Chemistry), propanal (\geq 99%, Acros Organics), and 1-propanol (\geq 99.5%, Sigma Aldrich) were purified with successive freeze–pump–thaw cycles using liquid nitrogen.

Gas phase mass spectra of the four molecules obtained with our system are given in the Supporting Information. These spectra were the basis for using the following mass-to-charge ratios as most characteristic for each molecule: 1-propanol (m/m)z = 31 amu), acrolein (m/z = 56 amu), 2-propenol (m/z = 57amu), and propanal (m/z = 58 amu). The m/z = 31 amu peak for 1-propanol was considerably more intense than the masses for the other molecules at a given pressure so that in some cases, the raw 1-propanol TPRS signal had to be scaled by a different factor for comparison with the other molecules. The TPR spectra were deconvoluted to account for mass fragmentation overlap and further corrected for mass fragment yield, ionization efficiency, gain from the electron multiplier, and quadrupole transmission.²⁴ A detailed explanation of these TPR corrections is given in the Supporting Information. A linear heating rate of 1 K/s was used to acquire TPRS/TPD

We have previously characterized the Pd/Ag(111) SAA surface using RAIRS and TPD of adsorbed CO.²⁰ The RAIRS results showed that CO adsorbs only on Pd atop sites at low Pd coverages, whereas at higher Pd coverages, CO adsorption at Pd bridge sites was detected. This allowed us to determine the Pd coverage at which the transition from isolated Pd atoms to Pd aggregates occurred. The CO TPD peak areas were used to quantify the low Pd coverages. This was based on calibrating the CO TPD peak area for a known high Pd coverage measured with Auger electron spectroscopy.

RESULTS

We previously showed that the hot filament of our ion gauge could be used to dose the Ag(111) surface with atomic hydrogen, which bypasses the high energy barrier for dissociation of molecular hydrogen on Ag(111). TPR spectra following adsorption of atomic hydrogen on Ag(111) are shown in Figure 1. The recombinative desorption of H_2 is

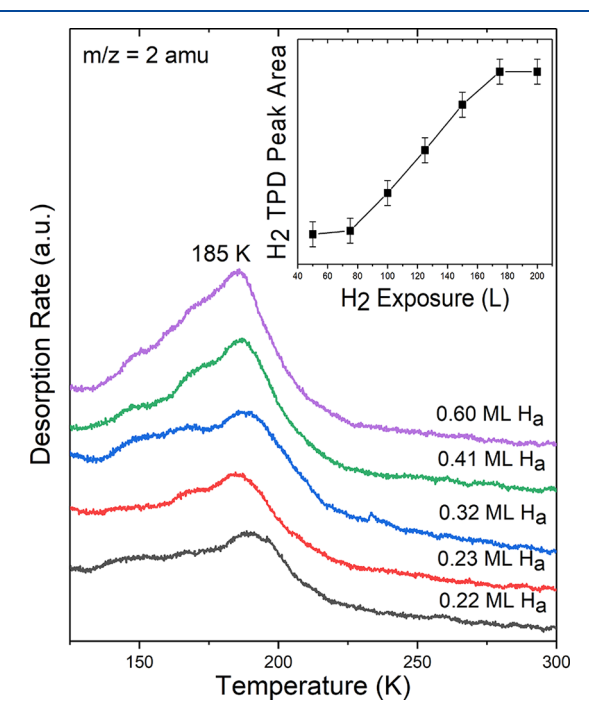


Figure 1. TPR results for the recombination of atomic H to form and desorb H_2 . The Ag(111) surface was exposed to H_2 with the ion gauge on, which dissociates some of the H_2 to atomic hydrogen. The indicated coverages are based on peak areas and an assumption of a saturation coverage of atomic H of 0.6 ML. The inset of peak area versus exposures shows that saturation coverage is achieved.

observed at 185 K. The saturation coverage of atomic hydrogen on Ag(111) has previously been shown to be approximately 0.6 monolayer (ML). 25,26 Therefore, we assume that a saturation coverage of 0.6 ML is reached when the TPR peak areas become constant after a 170 L (Langmuir) $\rm H_2$ exposure with the ion gauge on, where 1 L = 1 \times 10 $^{-6}$ Torr s. The results in Figure 1 reveal that $\rm H_2$ desorption from Ag(111) extends up to at least 250 K. Although the $\rm H_2$ TPR peak areas can be used to determine the absolute coverage of H when the surface is exposed only to hydrogen, when hydrogen exposure occurs after acrolein adsorption, this is no longer the case. Therefore, $\rm H_2$ exposures in L units with the ion gauge on are given for all subsequent TPR results.

Figure 2 shows TPD results for acrolein, 2-propenol, propanal, and 1-propanol on Ag(111). The coverages were determined based on separate studies of TPD peak areas as a function of exposure. One ML was taken as the area just before the appearance of a lower temperature multilayer desorption peak. Acrolein desorbs at 169 K, slightly higher than that of propanal at 164 K. 2-Propenol and 1-propanol show higher desorption peaks at 204 and 211 K, respectively. For 1-propanol, a higher temperature shoulder is observed. Other results reveal that this shoulder saturates at low coverages and is likely due to stronger adsorption at defects sites. Defect-site

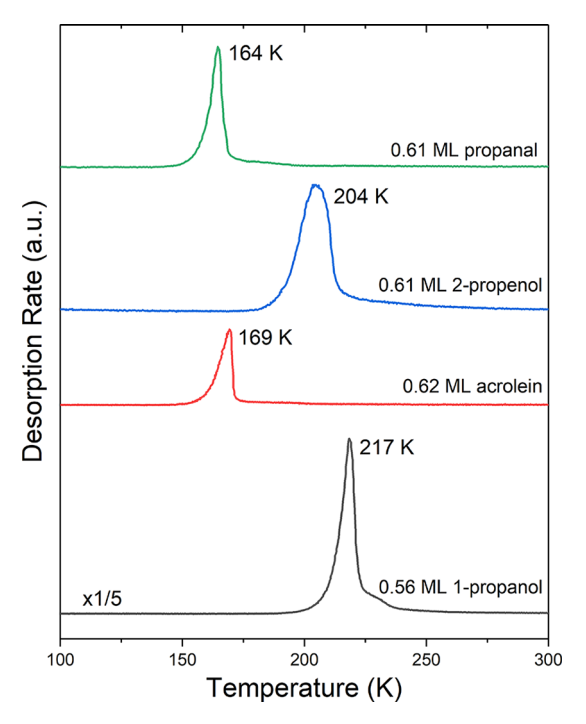


Figure 2. TPD spectra of 0.56 ML of 1-propanol, 0.62 ML of acrolein, 0.61 ML of 2-propenol, and 0.61 ML of propanal on Ag(111). The mass-to-charge ratio measured for each gas was 31, 56, 57, and 58 amu, respectively. The propanol signal was scaled by 1/5 because the mass 31 peak is large relative to the peaks used to monitor the other molecules.

desorption is not seen for the other molecules presumably because their binding to defects sites is not appreciably stronger than binding to the terrace sites.

Figure 3 shows TPR results for approximately 1 ML of acrolein at a full scale on Ag(111) and at an expanded scale with increasing Pd coverage. As Pd constitutes less than 1% of the surface, the majority of acrolein is adsorbed at Ag sites and desorbs at 170 K. However, a second peak at 250 K grows with increasing Pd coverage. The linear relationship between the 250 K peak area and Pd coverage confirms that acrolein desorbs from Pd sites at a higher temperature than from Ag sites

The hydrogenation of acrolein on Ag(111) was studied at three acrolein coverages (0.17, 0.29, and 0.62 ML) and four $\rm H_2$ exposures (50, 200, 500, and 1000 L) using TPRS. The TPR spectra for 0.17 ML of acrolein followed by 50 and 1000 L of $\rm H_2$ are shown in Figure 4.

The TPR spectra of 0.17 ML of acrolein followed by 50 L H₂ (Figure 4a) primarily show desorption of unreacted acrolein. 2-Propenol has a desorption peak at 295 K, while propanal interestingly shows four desorption peaks at 160, 248, 294, and 402 K. 1-Propanol shows a small desorption peak at 227 K. By increasing the hydrogen exposure to 1000 L (Figure 4b), a second high-temperature desorption peak is observed for 2-propenol while the four desorption peaks for propanal significantly increase in intensity. 1-Propanol also shows increased desorption at 164, 194, and 239 K. As the hydrogenation products show higher desorption temperatures than for the pure compounds on Ag(111) in Figure 2, these results indicate reaction-limited desorption. Reaction-limited desorption was also observed by Brandt et al., although they did not show TPRS results above 380 K, and the 310 and 367

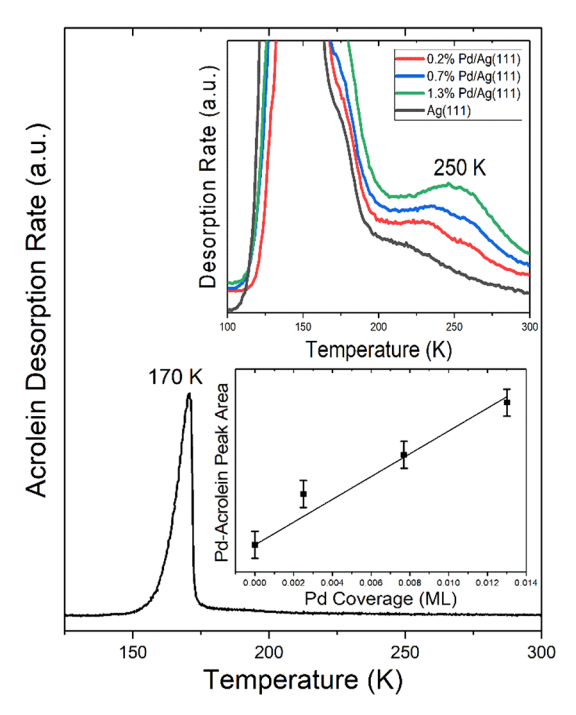


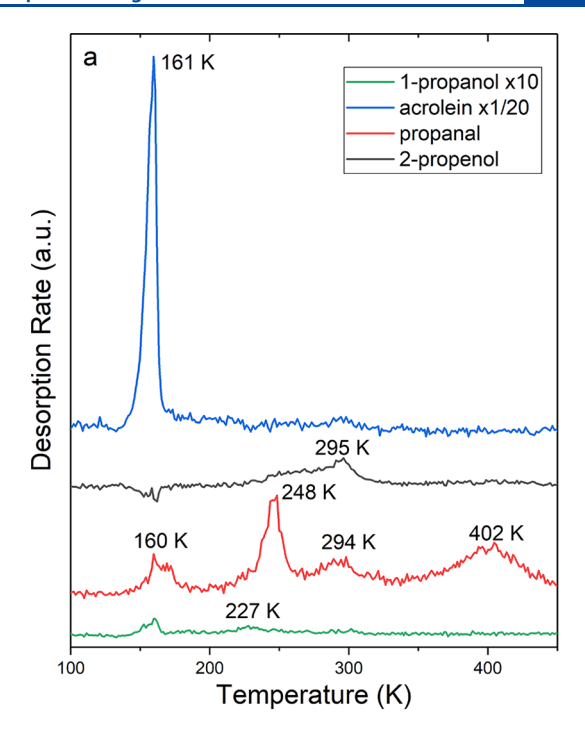
Figure 3. TPD spectra of approximately 1 ML of acrolein on Ag(111) (black) and on Pd/Ag(111) (inset) with increasing Pd coverage. The bottom inset is a plot of acrolein–Pd TPD peak areas versus Pd coverage.

K propanal desorption peaks were not apparent in their results. 14

The percent conversion of acrolein and percent selectivity toward each hydrogenation product are shown in Figure 5. Overall, the percent conversion increases with increasing $\rm H_2$ exposure. For 0.17 ML of acrolein, a maximum conversion was reached at 57% for 500 L of $\rm H_2$. Increasing the acrolein coverage to 0.29 and to 0.62 ML gave the highest conversions using 1000 L of $\rm H_2$ of 39 and 25%, respectively. However, since our interest was on selectivity to 2-propenol, we did not determine if higher conversions could be achieved for even higher $\rm H_2$ exposures.

The selectivity toward 2-propenol was the highest (19%) for the lowest acrolein coverage (0.17 ML). For the three acrolein coverages, the selectivity to 2-propenol was the highest for 50 L of $\rm H_2$ and decreased with increasing hydrogen exposure. The selectivity to propanal increases from 80% for 50 L of $\rm H_2$ to 90% for 200, 500, and 1000 L of $\rm H_2$. In all cases, the selectivity to the fully hydrogenated product, 1-propanol, was only 1%.

Figure 6 shows TPR spectra of 0.17 ML of acrolein followed by 50 L of H₂ on the 0.9% Pd/Ag(111) SAA surface. The desorption peaks for propanal and 1-propanol are significantly more intense than on the Ag(111) surface as seen in Figure 4a for the same acrolein coverage and hydrogen exposure. Compared to the Ag(111) surface, no desorption peaks are observed above 300 K for the Pd/Ag(111) SAA surface. The Pd atoms therefore alter the reaction pathway such that hydrogenation to propanal occurs at lower temperatures than on Pd-free Ag(111). We have previously shown that the Pd/Ag(111) alloyed surface undergoes Pd diffusion above 350 K to produce a capped Ag/Pd/Ag/(111) surface for low Pd coverages, in agreement with the work of van Spronsen et al. Therefore, at the final temperature in the TPR



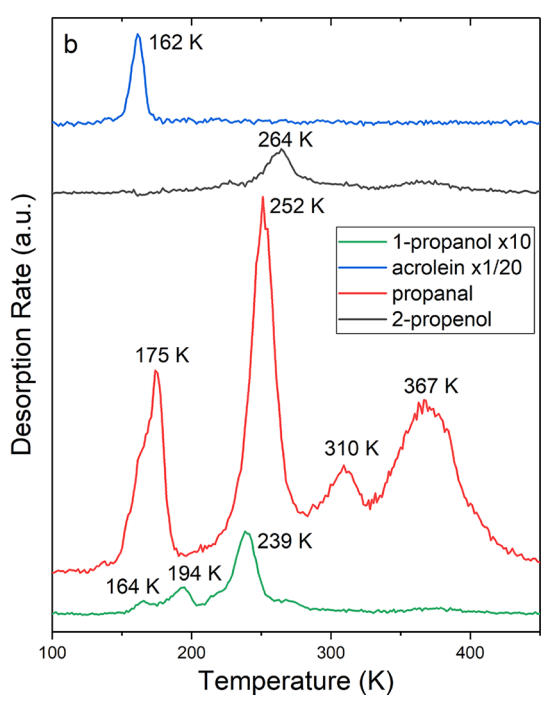


Figure 4. (a) TPR spectra after adsorption of 0.17 ML of acrolein on Ag(111) followed by exposure to 50 L of H_2 and (b) to 1000 L of H_2 . The m/z = 56 amu (acrolein) and 31 amu (1-propanol) peaks are multiplied by 1/20 and 10, respectively.

experiment, the structure of the surface is likely quite different from the initial structure.

To verify that the Pd coverages used here correspond to a SAA with mainly isolated Pd atoms, we recorded the CO TPD results shown in Figure 7. In our previous study, ²⁰ we showed using both RAIRS and TPD of adsorbed CO that Pd aggregates begin to form for Pd coverages higher than about 1%. From that study, we know that the 262–280 K peak in Figure 7 corresponds to CO at Pd on-top sites. We attribute

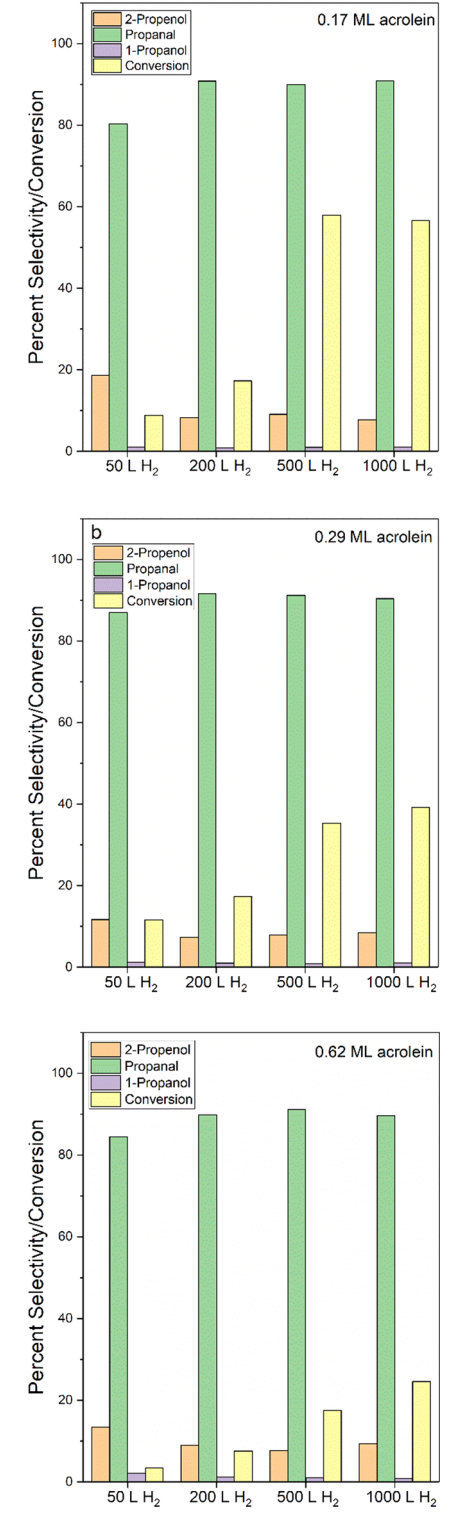


Figure 5. Percent conversion and selectivity to 2-propenol, propanal, and 1-propanol for (a) 0.17, (b) 0.29, and (c) 0.62 ML of acrolein on Ag(111) with increasing hydrogen exposure.

the lower temperature peak at 224 K to intermolecular repulsion between CO molecules sharing a small Pd aggregate, which leads to a lower desorption temperature. For much higher Pd coverages, a higher temperature CO desorption peak is seen. For example, for 13.5% Pd, the largest CO desorption peak is at 368 K,²⁰ comparable to the CO desorption temperature for low coverages of CO on Pd(111).²⁸

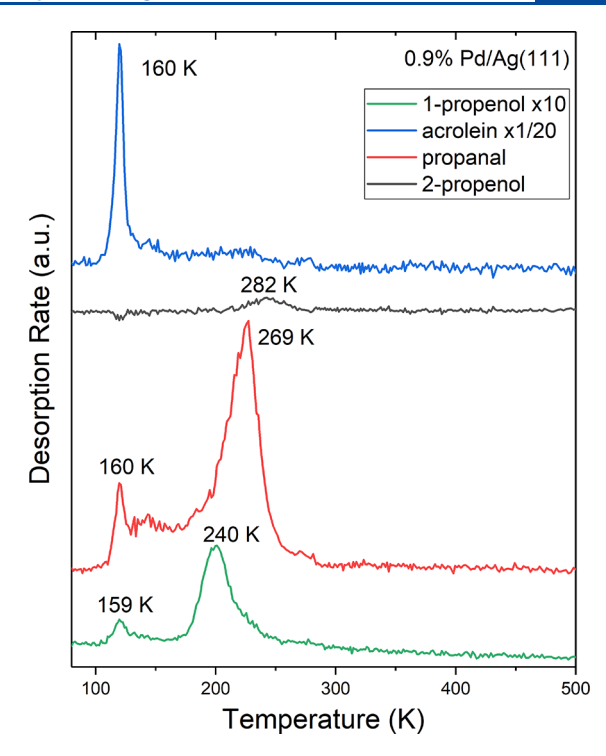


Figure 6. TPR spectra of 0.17 ML of acrolein after exposure to 50 L of $\rm H_2$ to 0.9% Pd/Ag(111) SAA. The m/z=56 and 31 amu peaks are multiplied by 1/20 and 10, respectively.

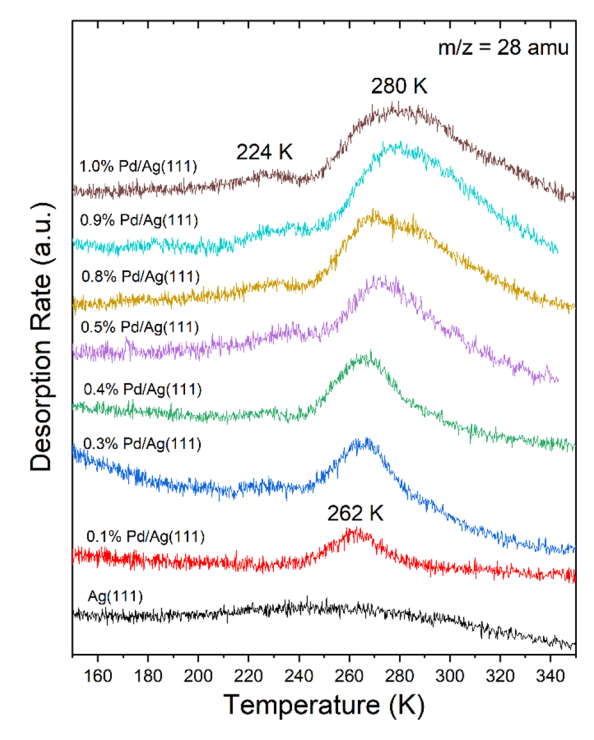


Figure 7. TPD spectra of 1 L of CO adsorbed on the Ag(111) and Pd/Ag(111) SAA surface with increasing Pd coverage from 0.1 to 1.0%. Pd was deposited onto the Ag(111) surface at 380 K.

In Figure 8, the conversion and selectivity for the Pd/Ag(111) SAA surface are shown and compared to Ag(111) for the adsorption of 0.17 ML of acrolein followed by a 50 L $\rm H_2$ exposure. The presence of single Pd atoms on the surface increases the conversion from 9% on Ag(111) to 15% on the 0.9% Pd/Ag(111) SAA surface. With increasing Pd coverage,

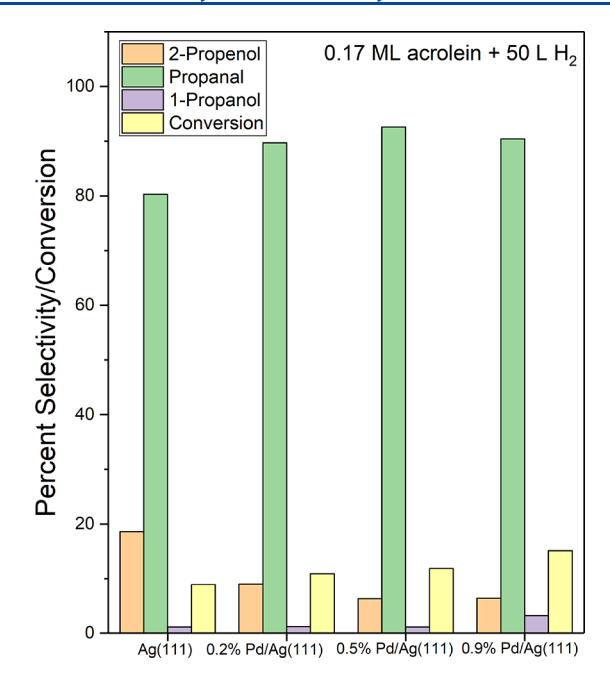


Figure 8. Percent conversion and selectivity to 2-propenol, propanal, and 1-propanol for 0.17 ML of acrolein followed by a 50 L H_2 exposure on Ag(111) and Pd/Ag(111) with increasing Pd coverage.

the selectivity to 2-propenol decreases from 19 to 6%, while selectivity to propanal increases from 80% on Ag(111) to 90–93% on the Pd/Ag(111) SAA surface. The selectivity toward the fully hydrogenated product, 1-propanol, increased to only 3% for the 0.9% Pd/Ag(111) SAA surface.

DISCUSSION

The dopant metal in SAAs can have a disproportionately large effect on hydrogenation reactions, and our results show this to be the case for acrolein hydrogenation over a Pd/Ag(111) SAA surface. Since it is known that hydrogen spillover does not occur on the Pd/Ag(111) SAA, 20,21 the role of the Pd goes beyond providing a low barrier site for dihydrogen dissociation. The reaction-limited desorption of the hydrogenation products implies that they form through further reaction of stable surface intermediates. It is plausible that partial hydrogenation of acrolein, C_3H_4O , to 2-propenol or propanal, C_3H_6O , occurs by adding one H atom to acrolein to produce a surface intermediate with a C_3H_5O stoichiometry. It is likely that the rate-limiting step in the appearance of propanal and 2-propenol is the addition of a second H atom to the C_3H_5O intermediate.

Lim et al. used DFT to explore possible reaction pathways for acrolein hydrogenation on a Ag(110) surface and on a Ag(111) surface containing sub-surface oxygen. They determined the adsorption energies of four possible C_3H_5O intermediates on these two surfaces. They found that 1-formylethyl was most stable and was the intermediate for propanal production. They identified two possible intermediates for 2-propenol formation, which they named hydroxyallyl and allyloxy, and determined that they have similar adsorption energies. Dostert et al. used RAIRS to study acrolein hydrogenation over a Pd(111) surface and identified the intermediate to 2-propenol formation as propenoxy, H_2C = $CHCH_2O$ -, with the C=C bond oriented perpendicular to the surface with a bond between the O atom and a Pd atom. This is similar to the allyloxy species identified by Lim et al. 29

With its upright geometry, propenoxy would be favored under the high coverage conditions in their experiment. They identified a second C_3H_5O moiety as oxopropyl, $H_3CHCCHO$, which is similar to the 1-formylethyl species identified by Lim et al.²⁹ Although our TPRS results can be interpreted in terms of stable surface intermediates, the technique does not provide information on their identities.

The origin on the large effect of a few surface Pd atoms on the hydrogenation properties of the Pd/Ag(111) SAA surface may lie in the stronger bonding of acrolein to Pd sites relative to Ag sites as revealed by our TPRS results. This conclusion is supported by DFT calculations. Ferullo et al. used DFT corrected for van der Waals interactions to show that isolated acrolein molecules have a binding energy to Ag(111) of -0.61 eV, whereas without correcting for van der Waals interactions the binding energy is only -0.06 eV. Aich et al. used DFT without van der Waals interactions to show that acrolein bonds through the C=C bond to an isolated Pd atom in a Ag(111) surface with a binding energy of -1.36 eV. Hydrogenation of an acrolein molecule bonded this way should occur at the C=C bond to form propanal. In this way, the presence of Pd should enhance selectivity to propanal, as observed.

We further speculate that Pd enhances hydrogenation of the C_3H_5O intermediates so that the hydrogenation reactions are completed at a lower temperature. If the intermediates migrated to Pd sites and reacted with hydrogen there to produce products that are immediately desorbed, additional intermediates would then migrate to the Pd sites to undergo hydrogenation. In this way, a few Pd atoms could completely suppress the higher-temperature pathway observed in Figure 4 for the Pd-free Ag(111) surface.

It might be possible to verify this mechanism by identifying the intermediates through *in situ* RAIRS studies of the sort conducted by Dostert et al. ³⁰ It is more likely, however, that the intermediates would never reach a high enough coverage to be detectable. *In situ* studies would also allow for a more direct comparison to the experimental results of Aich et al. ²³ over PdAg SAA nanoparticle catalysts. They used a H_2 /acrolein molar ratio of 20:1 with a flow rate of 3.2 μ L/min for acrolein. ²³ In the catalyst preparation method used by Aich et al., ²³ a distribution of particle sizes is usually obtained and with such a small fraction of Pd, some pure Ag particles were likely present. These would favor 2-propenol formation, contributing to the overall measured higher selectivity. This may partly explain the differences between their results and ours.

CONCLUSIONS

Under the most favorable conditions, a 19% selectivity was found for the partial hydrogenation of acrolein to 2-propenol on the Ag(111) surface. With just 0.2% Pd, the selectivity to 2-propenol decreased to only 9%. With increasing Pd coverage, the selectivity to 2-propenol decreased, while the selectivity to propanal and the percent conversion increased. All hydrogenation products desorb through reaction-limited kinetics, implying that the reaction proceeds through stable surface intermediates. Propanal is formed both above and below 300 K on Ag(111), but the higher temperature pathways are eliminated for the Pd/Ag(111) SAA surface.

ASSOCIATED CONTENT

Supporting Information

The Supporting Information is available free of charge at https://pubs.acs.org/doi/10.1021/acs.jpcc.0c08094.

MS of acrolein, 2-propenol, propanal, and 1-propanol and deconvolution and corrections for TPRS of acrolein hydrogenation (PDF)

AUTHOR INFORMATION

Corresponding Author

Michael Trenary — Department of Chemistry, University of Illinois at Chicago, Chicago, Illinois 60607, United States; orcid.org/0000-0003-1419-9252; Email: mtrenary@uic.edu

Authors

Mark Muir — Department of Chemistry, University of Illinois at Chicago, Chicago, Illinois 60607, United States

David L. Molina – Department of Chemistry, University of Illinois at Chicago, Chicago, Illinois 60607, United States

Arephin Islam – Department of Chemistry, University of Illinois at Chicago, Chicago, Illinois 60607, United States

Mohammed K. Abdel-Rahman — Department of Chemistry, University of Illinois at Chicago, Chicago, Illinois 60607, United States

Complete contact information is available at: https://pubs.acs.org/10.1021/acs.jpcc.0c08094

Notes

The authors declare no competing financial interest.

ACKNOWLEDGMENTS

This work was supported by a grant from the National Science Foundation, CHE-1800236.

REFERENCES

- (1) Claus, P. Selective Hydrogenation of α , β -Unsaturated Aldehydes and Other C=O and C=C Bonds Containing Compounds. *Top. Catal.* **1998**, *5*, 51–62.
- (2) Silva, E. A. P.; Carvalho, J. S.; Guimarães, A. G.; Barreto, R. D. S. S.; Santos, M. R. V.; Barreto, A. S.; Quintans-Júnior, L. J. The use of terpenes and derivatives as a new perspective for cardiovascular disease treatment: a patent review (2008–2018). Expert Opin. Ther. Pat. 2019, 29, 43–53.
- (3) Schwab, W.; Davidovich-Rikanati, R.; Lewinsohn, E. Biosynthesis of plant-derived flavor compounds. *Plant J.* **2008**, *54*, 712–732.
- (4) Delbecq, F.; Sautet, P. Competitive C=C and C=O Adsorption of α - β -Unsaturated Aldehydes on Pt and Pd Surfaces in Relation with the Selectivity of Hydrogenation Reactions: A Theoretical Approach. *J. Catal.* **1995**, *152*, 217–236.
- (5) Delbecq, F.; Sautet, P. A Density Functional Study of Adsorption Structures of Unsaturated Aldehydes on Pt(111): A Key Factor for Hydrogenation Selectivity. *J. Catal.* **2002**, 211, 398–406.
- (6) Marinelli, T. B. L. W.; Nabuurs, S.; Ponec, V. Activity and Selectivity in the Reactions of Substituted α , β -Unsaturated Aldehydes. *J. Catal.* **1995**, *151*, 431–438.
- (7) Esan, D. A.; Ren, Y.; Feng, X.; Trenary, M. Adsorption and hydrogenation of acrolein on Ru(001). *J. Phys. Chem. C* **2017**, *121*, 4384–4392.
- (8) Murillo, L. E.; Chen, J. G. A comparative study of the adsorption and hydrogenation of acrolein on Pt(111), Ni(111) film and Pt-Ni-Pt(111) bimetallic surfaces. *Surf. Sci.* **2008**, *602*, 919–931.
- (9) Esan, D. A.; Trenary, M. Selective hydrogenation of acrolein to propanal on a pseudomorphic Pt/Ru(001) bimetallic surface. *Top. Catal.* **2018**, *61*, 318–327.
- (10) Tuokko, S.; Pihko, P. M.; Honkala, K. First Principles Calculations for Hydrogenation of Acrolein on Pd and Pt: Chemoselectivity Depends on Steric Effects on the Surface. *Angew. Chem., Int. Ed.* **2016**, *55*, 1670–1674.

- (11) Bron, M.; Teschner, D.; Knop-Gericke, A.; Steinhauer, B.; Scheybal, A.; Hävecker, M.; Wang, D.; Födisch, R.; Hönicke, D.; Wootsch, A.; Schlögl, R.; Claus, P. Bridging the pressure and materials gap: in-depth characterisation and reaction studies of silver-catalysed acrolein hydrogenation. *J. Catal.* **2005**, 234, 37–47.
- (12) Claus, P.; Hofmeister, H. Electron Microscopy and Catalytic Study of Silver Catalysts: Structure Sensitivity of the Hydrogenation of Crotonaldehyde. *J. Phys. Chem. B* **1999**, *103*, 2766–2775.
- (13) Brandt, K.; Chiu, M. E.; Watson, D. J.; Tikhov, M. S.; Lambert, R. M. Adsorption Geometry Determines Catalytic Selectivity in Highly Chemoselective Hydrogenation of Crotonaldehyde on Ag(111). J. Phys. Chem. C 2012, 116, 4605–4611.
- (14) Brandt, K.; Chiu, M. E.; Watson, D. J.; Tikhov, M. S.; Lambert, R. M. Chemoselective Catalytic Hydrogenation of Acrolein on Ag(111): Effect of Molecular Orientation on Reaction Selectivity. *J. Am. Chem. Soc.* **2009**, *131*, 17286–17290.
- (15) Fujii, S.; Osaka, N.; Akita, M.; Itoh, K. Infrared Reflection Absorption Spectroscopic Study on the Adsorption Structures of Acrolein on an Evaporated Silver Film. *J. Phys. Chem.* **1995**, *99*, 6994–7001.
- (16) Akita, M.; Osaka, N.; Itoh, K. Infra-red reflection absorption spectroscopic study on adsorption structures of acrolein on polycrystalline gold and Au(111) surfaces under ultra-high vacuum conditions. *Surf. Sci.* **1998**, *405*, 172–181.
- (17) Darby, M. T.; Stamatakis, M.; Michaelides, A.; Sykes, E. C. H. Lonely Atoms with Special Gifts: Breaking Linear Scaling Relationships in Heterogeneous Catalysis with Single-Atom Alloys. *J. Phys. Chem. Lett.* **2018**, *9*, 5636–5646.
- (18) Kyriakou, G.; Boucher, M. B.; Jewell, A. D.; Lewis, E. A.; Lawton, T. J.; Baber, A. E.; Tierney, H. L.; Flytzani-Stephanopoulos, M.; Sykes, E. C. H. Isolated Metal Atom Geometries as a Strategy for Selective Heterogeneous Hydrogenations. *Science* **2012**, 335, 1209–1212.
- (19) Kruppe, C. M.; Krooswyk, J. D.; Trenary, M. Selective hydrogenation of acetylene to ethylene in the presence of a carbonaceous surface layer on a Pd/Cu(111) single-atom alloy. *ACS Catal.* **2017**, *7*, 8042–8049.
- (20) Muir, M.; Trenary, M. Adsorption of CO to Characterize the Structure of a Pd/Ag(111) Single-Atom Alloy Surface. *J. Phys. Chem.* C **2020**, *124*, 14722–14729.
- (21) O'Connor, C. R.; Duanmu, K.; Patel, D. A.; Muramoto, E.; van Spronsen, M. A.; Stacchiola, D.; Sykes, E. C. H.; Sautet, P.; Madix, R. J.; Friend, C. M. Facilitating hydrogen atom migration via a dense phase on palladium islands to a surrounding silver surface. *Proc. Natl. Acad. Sci. U. S. A.* **2020**, *117*, 22657.
- (22) Lim, J. S.; Vandermause, J.; van Spronsen, M. A.; Musaelian, A.; Xie, Y.; Sun, L.; O'Connor, C. R.; Egle, T.; Molinari, N.; Florian, J.; et al. Evolution of Metastable Structures at Bimetallic Surfaces from Microscopy and Machine-Learning Molecular Dynamics. *J. Am. Chem. Soc.* 2020, *142*, 15907–15916.
- (23) Aich, P.; Wei, H.; Basan, B.; Kropf, A. J.; Schweitzer, N. M.; Marshall, C. L.; Miller, J. T.; Meyer, R. Single-Atom Alloy Pd-Ag Catalyst for Selective Hydrogenation of Acrolein. *J. Phys. Chem. C* **2015**, *119*, 18140–18148.
- (24) Ko, E. I.; Benziger, J. B.; Madix, R. J. Reactions of methanol on W(100) and W(100)- (5×1) C surfaces. *J. Catal.* **1980**, *62*, 264–274.
- (25) Lee, G.; Sprunger, P. T.; Okada, M.; Poker, D. B.; Zehner, D. M.; Plummer, E. W. Chemisorption of Hydrogen on the Ag(111) Surface. *J. Vac. Sci. Technol., A* **1994**, *12*, 2119–2123.
- (26) Lee, G.; Plummer, E. W. Interaction of hydrogen with the Ag(111) surface. *Phys. Rev. B* **1995**, *51*, 7250–7261.
- (27) van Spronsen, M. A.; Daunmu, K.; O'Connor, C. R.; Egle, T.; Kersell, H.; Oliver-Meseguer, J.; Salmeron, M. B.; Madix, R. J.; Sautet, P.; Friend, C. M. Dynamics of Surface Alloys: Rearrangement of Pd/Ag(111) Induced by CO and O₂. *J. Phys. Chem. C* **2019**, 123, 8312–8323.
- (28) Guo, X. C.; Yates, J. T. Dependence of Effective Desorption Kinetic Parameters on Surface Coverage and Adsorption Temperature CO on Pd(111). *J. Chem. Phys.* **1989**, *90*, *6761*–*6766*.

- (29) Lim, K. H.; Mohammad, A. B.; Yudanov, I. V.; Neyman, K. M.; Bron, M.; Claus, P.; Rösch, N. Mechanism of Selective Hydrogenation of α,β -Unsaturated Aldehydes on Silver Catalysts: A Density Functional Study. *J. Phys. Chem. C* **2009**, *113*, 13231–13240.
- (30) Dostert, K.-H.; O'Brien, C. P.; Ivars-Barceló, F.; Schauermann, S.; Freund, H.-J. Spectators Control Selectivity in Surface Chemistry: Acrolein Partial Hydrogenation Over Pd. J. Am. Chem. Soc. 2015, 137, 13496–13502.
- (31) Ferullo, R. M.; Branda, M. M.; Illas, F. Structure and stability of acrolein and allyl alcohol networks on Ag(111) from density functional theory based calculations with dispersion corrections. *Surf. Sci.* **2013**, *617*, 175–182.